coatings

MDPI

Article

Enhancing Biodegradable Packaging: The Role of Tea Polyphenols in Soybean Oil Body Emulsion Films

Jie Sun, Luyang Wang, Han Chen and Guoyou Yin *

College of Life Science and Engineering, Henan University of Urban Construction, Pingdingshan 467036, China; 30110503@huuc.edu.cn (J.S.)
* Correspondence: 30110605@huuc.edu.cn; Tel.: +86-853-7506-086

Abstract: To address the increasingly diverse demands for biodegradable packaging materials, such as for their physical properties and antioxidant properties, this study incorporated tea polyphenols (TPs) into soybean oil body emulsions (SOBs) and added a certain proportion of sodium alginate (SA) and octenyl succinic starch sodium (SSOS) to prepare a biodegradable soybean oil body–tea polyphenol (ST) emulsion film. The study systematically evaluated the effects of different concentrations of TP (0–6 wt.%) on the structure, physicochemical properties, antioxidant activity, and antibacterial activity of ST films. The results showed that the physical properties, such as tensile strength and elongation at break, of the films increased significantly with the addition of TP, and the antioxidant and antibacterial activity also increased with the increase in TP concentration. When TP concentration was 2.5 wt.%, the barrier properties of the film (ST-2.5) significantly improved ($p < 0.05$), while water content and water solubility decreased. The Fourier transform infrared spectroscopy, scanning electron microscopy, and thermogravimetric analysis results showed that the structure of ST films became tighter at this point. The addition of TP also affected the sensory properties of ST films, such as with an increase in the opacity of the film. Compared with the control, the light transmittance of ST-6.0 decreased by 23.68% at a wavelength of 600 nm, indicating a significant reduction in film transparency. Moreover, the biodegradability test showed that ST films have good degradability. Therefore, the ST film, as a functional edible film, has broad application prospects in the food packaging industry.

Keywords: soybean oil bodies (SOBs); edible film; tea polyphenols; polysaccharide; antibacterial activity; biodegradability

Academic Editor: Rafael L. Quirino

Received: 12 August 2024
Revised: 23 January 2025
Accepted: 28 January 2025
Published: 2 February 2025

Citation: Sun, J.; Wang, L.; Chen, H.; Yin, G. Enhancing Biodegradable Packaging: The Role of Tea Polyphenols in Soybean Oil Body Emulsion Films. *Coatings* **2025**, *15*, 162. https://doi.org/10.3390/coatings15020162

1. Introduction

Synthetic plastic polymer films are widely used in food packaging. However, they have significant negative impacts on the environment due to their non-recyclability, difficulty in degradation, and generation of microplastics during decomposition [1]. To alleviate environmental pollution problems and with the increasing attention paid to food safety, edible films made from natural biopolymers such as proteins, polysaccharides, and lipids have become a research focus in the field of food packaging. Compared with films made from a single ingredient, composite edible films made from two or more materials, such as the combination of proteins with excellent mechanical properties and polysaccharides with excellent gas barrier properties after film formation, can better increase the mechanical and barrier properties of the film [2]. Such composite films are more popular in research and practical applications. However, both proteins and polysaccharides have poor water vapor barrier properties, which limits their application in food packaging [3].

Numerous studies have shown that adding lipids can effectively enhance the hydrophobicity and water vapor barrier properties of edible films, thereby reducing water loss and improving tensile properties [4]. Some researchers have dispersed lipid materials into the film matrix to form an emulsion, which not only makes the emulsion film easy to process but also achieves complementary advantages among various film base materials [5,6]. Xu et al. have studied the effect of stable clove essential oil Pickering emulsion incorporating corn protein on the structure and properties of chitosan film. They have shown that blending clove essential oil Pickering emulsion into edible films can significantly reduce water vapor permeability. Therefore, dispersing lipid materials into the water-based film matrix to form an emulsion is an effective way to improve the water resistance of edible films [7]. Currently, most research has focused on developing functional emulsion films, combining plant essential oils and edible films with good water resistance, antibacterial, and antioxidant effects. However, there are some drawbacks to these emulsion films. Firstly, plant essential oils are incompatible with the film matrix and require the addition of emulsifiers and high-energy homogenization processes, making the production process complex [8]. Secondly, the addition of high concentrations of plant essential oils can alter the taste of food and affect the transparency of the film [9].

Plant oil bodies are spherical droplets with a particle size of about 0.5 to 2 μm. Plant oil bodies can effectively solve the emulsification- and flavor-related issues of plant essential oils. Plant seeds utilize oil bodies as a storage site for lipids, which serves as a source of energy for seed germination and seedling growth. The internal liquid matrix of the oil bodies is triacylglycerol, and the surface is covered by a monolayer of phospholipids and endogenous proteins to form a biological membrane [10,11]. Soybean, as an important oil crop, has been extensively studied for its soybean oil body (SOB). SOBs are a natural source of emulsifiers that can disperse in water and form natural water-in-oil emulsions [12]. The formation of natural emulsions does not require additional emulsifiers or high-energy homogenization processes, making SOBs an ideal material for preparing emulsion films. Some research has been conducted on using oil bodies to prepare edible films. Wang has studied the film-forming properties of SOBs and applied them to the preservation of freshly cut potatoes [13]. Our preliminary research has also found that SOBs perform well in cross-linked matrices of sodium alginate and carboxymethyl cellulose, with improved stretch and barrier properties [14]. However, despite being a good substrate for preparing packaging films, SOBs still have some disadvantages, such as the lack of antibacterial and antioxidant activity, which limits their direct application in active packaging. Incorporating natural functional substances into SOB emulsion films is a feasible way to solve these issues. Currently, some natural preservatives extracted from plants have been well-applied in active films. Tea polyphenol (TP) is the primary active compound in tea, exhibiting significant biological activities such as antiviral, antibacterial effects, and antioxidant effects, achieved through the capture of reactive oxygen species and chelation of metal ions [15,16]. TP has good antioxidant activity and non-toxic properties in various food model systems, which makes it a promising natural preservative and antioxidant with wide applications. In recent years, TP has been successfully combined with natural polysaccharides such as starch, gelatin, and chitosan to prepare bioactive films, such as edible films. TP addition can improve the transparency, mechanical strength, and antioxidant properties of edible films while inhibiting the growth of bacteria and fungi, with significant application value in food preservation and packaging [17]. Zhou et al. added TP to chitosan and bacterial cellulose to prepare edible films with antibacterial and antioxidant functions. They found that when the polyphenol content was 8 wt.%, the film played an important role in prolonging the shelf life of the grass carp [18]. There are currently few reports on SOB emulsion films, and there is also a lack of research on the behavior of bioactive substances in SOB emulsion films.

Sodium alginate (SA) and octenyl succinic starch sodium (SSOS) can stabilize oil body emulsions, and edible films prepared from these two polysaccharides have good mechanical and barrier properties [19]. Therefore, taking into account the current trends in food packaging development, this study used a soybean oil body emulsion as a film-forming matrix, and added sodium alginate and octenyl succinic starch sodium into the soybean oil body emulsion. Different concentrations of tea polyphenols were added to the emulsion system to prepare edible active films, and the effects of tea polyphenols on the structure, physicochemical properties, antioxidant activity, and antibacterial activity of the emulsion film were systematically studied. The aim is to develop biodegradable packaging materials with good functional properties and to provide ideas for finding and developing even better membrane materials.

2. Materials and Methods

2.1. Materials

Soybeans were obtained from Dexinquan supermarket (Pingdingshan, China). TP, SA, and SSOS were provided by Henan Qihuali Biotechnology Co., Ltd. (Zhengzhou, China). Glycerin,2,2-diphenyl-1-picrylhydrazy(DPPH),2,2-azinobis-(3-ethylbenzothiazoline-6-sulfonic acid) (ABTS) and glycerin were purchased by Beijing Solaibao Technology Co., Ltd. (Beijing, China). *Escherichia coli* (ATCC25922) and *Staphyloccocus aureus* (ATCC29213) were stored at the Laboratory of Food Processing and Components, Henan University of Urban Construction. All other reagents were of analytical grade.

2.2. Preparation of ST Films

The soybean oil body was dispersed in distilled water to prepare an oil body emulsion (1.5 g/100 mL). Then, 0.5 g of SSOS and 1 g of SA were dissolved in the oil body emulsion, and glycerol (1.2 g/100 mL) was added. The mixture was stirred for 30 min at 60 °C until completely dissolved. Then, 0 wt.%, 1.5 wt.%, 2.5 wt.%, 4.0 wt.%, and 6.0 wt.% TP were added to prepare membrane solutions, named ST-0, ST-1.5, ST-2.5, ST-4.0, and ST-6.0, respectively. After defoaming for 12 h, 60 mL of the membrane solution was poured into each 120 mm diameter dish, dried at 60 °C in an oven for 8 h, and then equilibrated in the closed oven for 12 h before peeling off and being used for subsequent experiments.

2.3. Characterization of ST Films

2.3.1. Thickness

A spiral micrometer was used to measure the thickness of ST films in 10 random locations per sample and the measurements were taken three times in each location.

2.3.2. Mechanical Property

The tensile strength (TS) and elongation at break (EB) of ST films were evaluated using a TMS-PRO texture analyzer (FTC, VA, USA). Film samples were cut into fixed-size pieces (10 mm × 70 mm) and loaded onto the device at a speed of 0.5 mm/s. TS and EB were calculated as follows:

$$\mathrm{TS} = \frac{\mathrm{F}}{\mathrm{T}\cdot\mathrm{W}}$$

$$\mathrm{EB}(\%) = \frac{L - L_0}{L_0} \times 100\%$$

Here, F denotes the maximum tensile force (N) at the sample break, T denotes film thickness (m), and W denotes film width (m). L denotes the elongation length of film (m) when it breaks, and L_0 represents the original length (m) of film.

2.3.3. Water Sensitivity

The moisture content (MC) can be measured by directly drying the film [20]. The films were cut into a square shape with a size of 30 mm × 30 mm and weighed as m_0. They were then dried in an oven at 105 °C until a constant weight was obtained and weighed as m. The formula for calculating the MC of the film was as follows:

$$\text{Moisture content}(\%) = \frac{m_0 - m}{m_0} \times 100\%$$

Here, m_0 represents the initial weight of film, and m represents the weight of film after drying to a constant weight.

Water solubility is the weight percentage of soluble components in a film sample [21]. The treatment of the film sample is the same as that of water solubility and the dry weight after drying at 105 °C was recorded as w_0. After drying, the film samples were soaked in 50 mL of deionized water at 25 °C for 1 h. Then, they were dried at 105 °C to a constant weight to obtain the final dry weight (w). The formula for calculating water solubility was as follows:

$$\text{Water solubility}(\%) = \frac{w_0 - w}{w_0} \times 100\%$$

2.3.4. Color Parameters

The color parameters of the film were measured using a colorimeter (WSC-S, Shanghai Yidian Physical Optical Instrument Co., Ltd., Shanghai, China) according to the CIE $L^*a^*b^*$ system (L^* (lightness), a^* (green to red), and b^* (blue to yellow)) and using a standard whiteboard as a comparison. The total color difference (ΔE) and chromaticity (c) were calculated using the following equations:

$$\Delta E = \sqrt{\Delta a^2 + \Delta b^2 + \Delta L^2}$$

$$c = \sqrt{a^2 + b^2}$$

where $\Delta a = a^*_{\text{standard}} - a^*_{\text{sample}}$; $\Delta b = b^*_{\text{standard}} - b^*_{\text{sample}}$; $\Delta L = L^*_{\text{standard}} - L^*_{\text{sample}}$. The L^*, a^*, and b^* values of the standard whiteboard were measured as follows: $L^*_{\text{standard}} = 98.24 \pm 0.03$; $a^*_{\text{standard}} = 1.01 \pm 0.01$; $b^*_{\text{standard}} = -1.56 \pm 0.02$.

2.3.5. Opacity and Transmittance

The determination of film opacity and transmittance was carried out according to the method proposed by Wu et al., with some modifications [22]. The films were cut into rectangular pieces (30 mm × 10 mm) and attached to Petri dishes, and their absorbance at a wavelength of 600 nm was measured using a spectrophotometer (T60, UV/Vis spectrometer, PG Instruments Ltd., Lutterworth, UK). Empty Petri dishes were used as blank samples. The opacity and transmittance of films were calculated using the following formulas:

$$\text{Opacity} = \frac{A_{600}}{d}$$

Here, A_{600} represents the absorbance at 600 nm, and d represents the thickness of films (mm).

The transmittance (T%) of the film was calculated using the following formula:

$$T(\%) = 0.1^{\text{A}} \times 100\%$$

Here, A is the absorbance of films at 600 nm, and T is the transmittance of films.

2.3.6. Barrier Property

The barrier properties of films were evaluated by their diffusion characteristics, specifically water vapor permeability (WVP) and oxygen permeability (OP). WVP was measured using the method of Tan et al. [23,24]. In a beaker, 2 g of silica gel was weighed to achieve 0% relative humidity. Then, the beaker was covered with the film and weighed again as w_0. After being left at room temperature for 24 h, the weight was measured again as w. The formula for calculating water vapor permeability is as follows:

$$\mathrm{WVP} = \frac{\Delta \mathrm{m} \times \mathrm{L}}{\mathrm{t} \times \mathrm{A} \times \Delta \mathrm{p}}$$

where t is the time (s), A is the measuring area (m^2), Δp is the water vapor pressure difference between the two sides of the film, Δm is the weight change in the glass bottle (g), and L is the thickness of the film (m).

The detection of oxygen permeability (OP) is based on an iron oxidation mechanism, following the method of Zhou et al. [18]. Sodium chloride (1.5 g), activated charcoal (1 g), and reduced iron powder (0.5 g) were added to a brown bottle with an open diameter of 2 cm. The film sample (with a permeable area of 3.1416×10^{-4} m^2) was then placed on top of the brown bottle, and the brown bottle with the film sample was placed in a dryer filled with saturated calcium chloride solution to achieve 90% relative humidity at 25 °C. The formula for calculating OP is as follows:

$$\mathrm{OP} = \frac{m - m_0}{t \times s}$$

where m_0 is the initial weight of the brown bottle (kg), m is the final weight of the brown bottle and the oxygen passing through the film (kg), t is the measuring time, and s is the area of the bottle covered by the film sample (m^2).

2.3.7. Fourier Transform Infrared (FT-IR) Analysis

The film samples were analyzed (20 mm × 20 mm) using a Fourier transform infrared spectrometer (PerkinElmer Spectrum, PerkinElmer Enterprise Management (Shanghai) Co., Ltd., Shanghai, China) [14]. The scanning range was 4000 cm^{-1} to 650 cm^{-1}, with a resolution of 4 cm^{-1}.

2.3.8. X-Ray Diffraction Analysis (XRD)

The freeze-dried ST film was placed in an X-ray diffraction instrument (Ultima IV, Rigaku Corporation, Tokyo, Japan). Cu-Kα radiation (λ = 1.542 Å) was used at 40 kV and 100 mA, with a scanning speed of 4°/min, a step size of 0.02, and diffraction angles (2θ) ranging from 5 to 50°.

2.3.9. Thermogravimetric Analysis

The thermal stability of the composite film was determined according to the method of Sun et al. [25]. The films were cut into small pieces, and 5 mg of the sample was weighed for the analysis. The sample was heated from 30 °C to 600 °C at a rate of 10 °C/min in a constant flow of nitrogen gas (20 mL/min).

2.3.10. Scanning Electron Microscopy (SEM)

The samples were frozen and fractured in liquid nitrogen and then coated with gold. They were then transferred to SEM (S-4800, Hitachi, Tokyo, Japan) and scanned at voltage of 3.0 kV.

2.3.11. Antioxidant Activity

Following the method of Kim et al., the antioxidant activity of the films was evaluated using DPPH and ABTS radical scavenging assays [26]. The film extract was prepared by taking 0.5 g of the film sample and adding it to 10 mL of deionized water, shaking and mixing for 24 h, and then centrifuging at 6000 rpm for 10 min. Supernatant was used for the determination of free radical scavenging activity.

DPPH Radical Scavenging Rate

The supernatant (50 μL) was mixed with 120 μL of DPPH solution (0.2 mmol/L DPPH in 95 vol.% ethanol), and the reaction was incubated in the dark at 25 °C for 30 min. Subsequently, the DPPH radical scavenging rate was calculated by measuring the absorbance at 517 nm with the following equation:

$$\text{DPPH radical scavening rate}(\%) = \frac{Abs_0 - Abs}{Abs} \times 100\%$$

where Abs_0 represents the absorbance of the control, and Abs represents the absorbance of the film sample.

ABTS Radical Scavenging Rate

Here, 7 mmol/L ABTS solution and 2.45 mmol/L potassium persulfate solution were prepared with 0.2 mol/L PBS (pH7.4) and mixed equal volumes (1:1) of the ABTS and potassium persulfate solutions; then, the mixture was reacted in the dark at 25 °C for 16 h. The dark solution was diluted with ethanol to obtain an ABTS-ethanol solution with an absorbance of 0.70 ± 0.02 at 734 nm. This was the ABTS radical cation (ABTS•+) preparation solution. A quantity of 30 μL of the sample solution was mixed with 170 μL of the ABTS-ethanol and the ABTS-ethanol solution was used as the control group. The results were calculated as the ABTS free radical scavenging rate (%) according to the following equation:

$$\text{ABTS radical scavening rate}(\%) = \frac{Abs_0 - Abs}{Abs_0} \times 100\%$$

where Abs_0 is the absorbance of the control, and Abs is the absorbance of the film sample.

2.3.12. Antibacterial Activity

The film (0.2 g) was immersed in 15 mL of meat peptone broth containing 100 μL of bacterial culture (10^5 CFU/mL) and incubated under constant temperature at 37 °C. Samples (1 mL) were taken at 12 h and 24 h, and their optical density was measured at 560 nm using a spectrophotometer (T60, UV/Vis spectrometer, PG Instruments Ltd., UK) [27].

2.3.13. Biodegradability

The biodegradability of ST films was evaluated using a soil burial test at 25 °C. A rectangular plastic container was filled with soil (50 mm depth) collected from beneath a tree. The film samples (30 mm × 30 mm) and plastic wrap (30 mm × 30 mm) were buried in the soil-filled plastic container, and water was sprayed onto the soil daily to maintain moisture [28]. The film samples were extracted from the soil and photographed to determine their biodegradability at intervals of 0, 3, 5, 9, and 11 days.

2.3.14. Statistical Analysis

All experiments were conducted in triplicate, and the results were presented as the mean ± standard deviation. The mean and standard deviation were calculated using GraphPad Prism 9.0. Statistical analysis was performed by ANOVA using IBM SPSS statistics, version 25 (IBM Inc., Armonk, NY, USA). $p < 0.05$ was considered as statistical significance.

3. Results and Discussion

3.1. Thickness Analysis

The addition of TP increased the solid content of the polymer matrix of the film, leading to a change in the thickness of the ST films [29]. Figure 1A showed that the thicknesses of ST films were between 0.12 mm and 0.14 mm, and there was no significant difference among the groups ($p > 0.05$). This may be because the amount of TP added to the film matrix was relatively low, and had little effect on the thickness of the ST film [17,30].

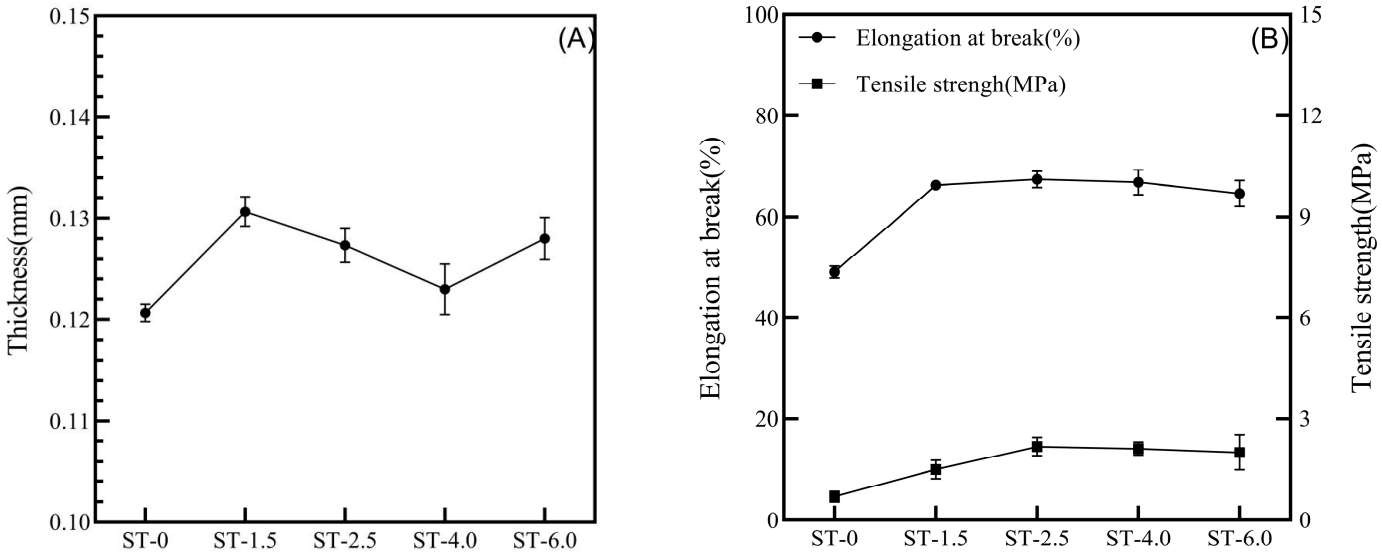

Figure 1. (**A**) Thickness of ST films; (**B**) elongation at break and tensile strength of ST films.

3.2. Mechanical Property Analysis

Figure 1B shows the mechanical properties of the ST film, including tensile strength (TS) and elongation at break (EB). It can be observed that the EB of ST films were between 49.06% and 67.36%, and TS values ranged from 0.69 MPa to 2.16 MPa. ST-2.5 had the highest values of EB and TS, which were 67.36% and 2.16 MPa ($p < 0.05$), respectively. This may be because the addition of TP caused stronger hydrogen bonding interactions between the hydroxyl groups in the ST films, thereby improving the mechanical properties [31]. However, when TP content reached 4.0 wt.%, the EB and TS of ST films began to decrease. Generally, when the oil exists in the form of emulsion droplets and a film is formed in the biopolymer, the film structure often becomes more flexible, with decreased rigidity. This is reflected in the increased toughness of the film; that is, an increase in EB [32]. However, a high TP concentration in the film may exist in the form of free particles, weaken its network structure, and disrupt the stable state of the SOB emulsion system, resulting in a decrease in EB and TS [33].

3.3. Water Sensitivity

As shown in Figure 2A, compared with the control group (ST-0), the water content of ST-1.5 and ST-2.5 decreased to 24.22% and 23.00% ($p < 0.05$), respectively. This change may be due to the binding of the phenolic hydroxyl group of TP with the hydroxyl groups of the SSOS, which reduced the hydroxyl groups exposed on the film and further reduced the water content of the film. The increase in the water content of ST-4.0 was due to the fact that TP is inherently more hydrophilic than SSOS. Therefore, when TP concentration reached a certain level, the water content of the film would also increase [34]. With the increase in TP content, the water solubility of ST films increased and showed concentration dependence. This may be due to the solubility of TP in water. After the addition of TP, the polymer network of the film was more easily decomposed when it came into contact with water, thus increasing the water solubility of the film [35].

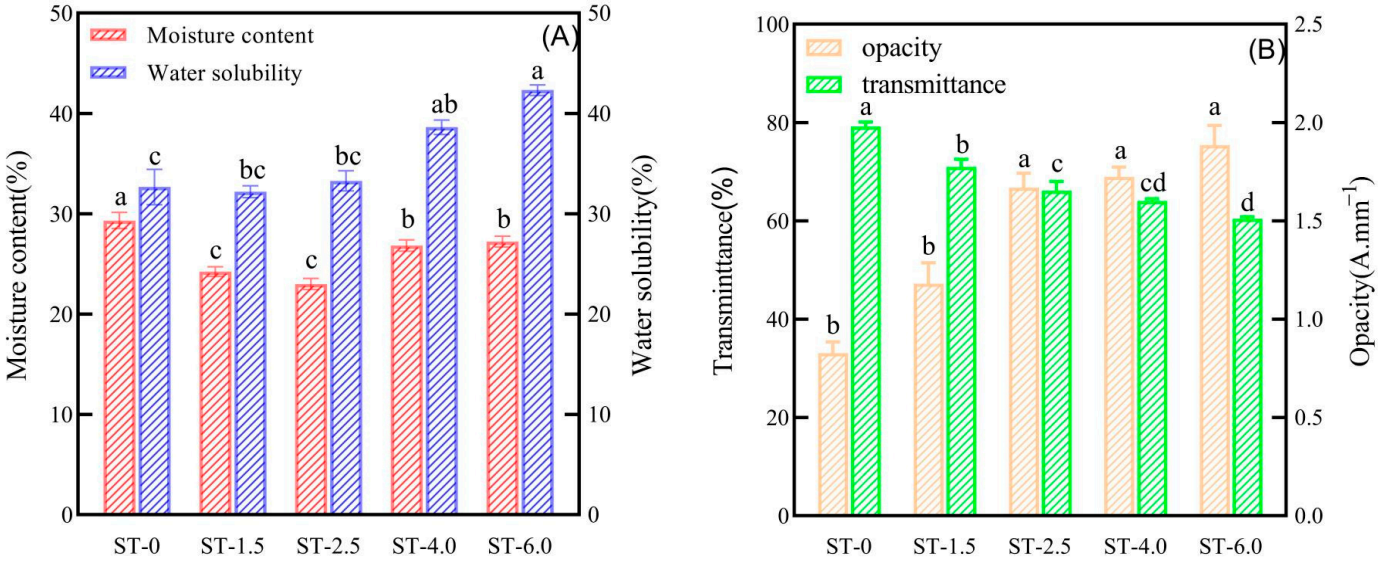

Figure 2. (**A**) Water content and solubility of ST films; (**B**) transmittance and opacity of ST films. Different lowercase letters in the same column indicate significant differences between groups ($p < 0.05$).

3.4. Colorimetric Analysis

Table 1 shows the effect of TP on the color of ST films. The addition of TP caused a decrease in the L^* value of the film, and ST-0 had the highest L value of 30.83 ± 0.34, indicating that the addition of TP decreased the lightness of the film, making it darker.

Table 1. The effect of the TP concentration on the color of films.

Films	L^*	a^*	b^*	ΔE	c
ST-0	67.41 ± 0.90 ^{a}	2.68 ± 0.03 ^{e}	2.29 ± 0.01 ^{e}	31.12 ± 0.92 ^{e}	3.52 ± 0.02 ^{e}
ST-1.5	60.21 ± 0.68 ^{b}	4.80 ± 0.01 ^{d}	16.04 ± 0.02 ^{d}	42.08 ± 0.80 ^{d}	16.74 ± 0.02 ^{d}
ST-2.5	59.08 ± 0.63 ^{bc}	5.85 ± 0.01 ^{c}	18.13 ± 0.02 ^{c}	44.10 ± 0.75 ^{c}	19.05 ± 0.02 ^{c}
ST-4.0	57.27 ± 0.39 ^{c}	7.28 ± 0.03 ^{b}	20.07 ± 0.01 ^{b}	46.75 ± 0.35 ^{b}	21.35 ± 0.01 ^{b}
ST-6.0	52.57 ± 1.25 ^{d}	10.96 ± 0.08 ^{a}	29.37 ± 0.03 ^{a}	56.05 ± 1.12 ^{a}	31.35 ± 0.04 ^{a}

Note: Significant differences are expressed by different letters (a–c) ($p < 0.05$). Different letters in the same column indicate significant differences ($p < 0.05$).

Moreover, with the increase in TP concentration, the a^* value of the film increased from 2.68 ± 0.03 to 10.96 ± 0.08, indicating that the ST films gradually became reddish. The a^* value of ST-0 was positive, reaching 2.68 ± 0.03, which may be due to the influence of the

color of the SOB on the film, which is milky white or slightly yellowish [36]. In addition, due to the inherent yellowish-brown color of TP, the b^*, ΔE, and c values of ST film showed an increasing trend, consistent with the results of Biao et al. [37].

3.5. Transmittance and Opacity

Transmittance, opacity, absorbance, and haze are important parameters that reflect the optical properties of materials and have been used to determine the transparency of food packaging materials. The most important indicators are transmittance and opacity [38,39]. After the addition of TP, the opacity of ST films significantly increased, from 0.81 ± 0.13 for ST-0 to 1.71 ± 0.27 for ST-6.0 ($p < 0.05$). This may be due to the structural heterogeneity of the film, having different refractive indices after adding TP, which enhances the phenomenon of light scattering [22]. In addition, with the increase in TP concentration, the transmittance of ST films decreased from (79.20 ± 1.55)% to (60.44 ± 0.71)%. Studies have shown that ST films containing TP have specific functions such as antioxidant and antibacterial activity, which can better protect food [40] (Figure 2B).

3.6. Barrier Property Analysis

Diffusion properties of film reflect its water blocking and antioxidant abilities, which are crucial for active packaging [41]. In general, SA and SSOS have a high hydrophilicity, which means that ST films will have a higher WVP value. However, based on the results in Figure 3A, ST-2.5 has a higher WVP value, and this may be attributed to the chemical bond formation between TP and the proteins outside the SOB, which created a more cohesive surface structure [42]. Therefore, adding a small amount of TP can help to reduce WVP to some extent. However, as TP is a naturally hydrophilic substance with a high concentration of hydrophilic groups, an increase in TP concentration will lower the water blocking ability of film [43]. With the change in TP concentration, the OP showed the same trend as WVP, with the oxygen permeability of ST-2.5 decreasing by 52.35% compared to the control group ($p < 0.05$) (Figure 3B).

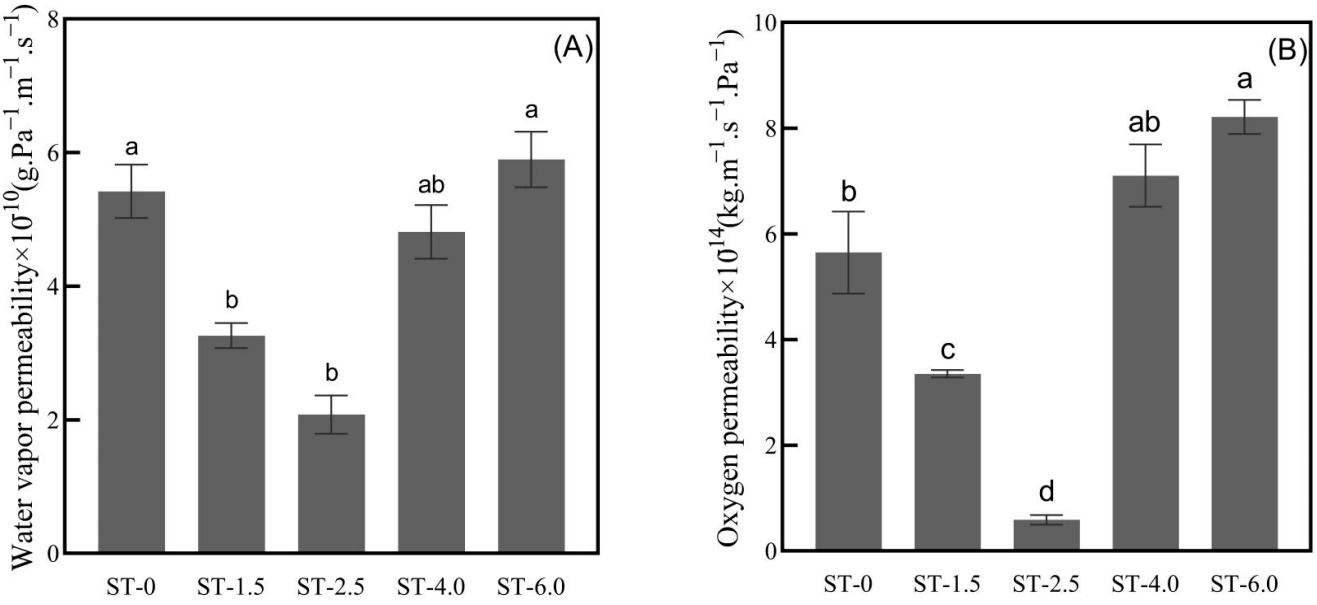

Figure 3. *Cont.*

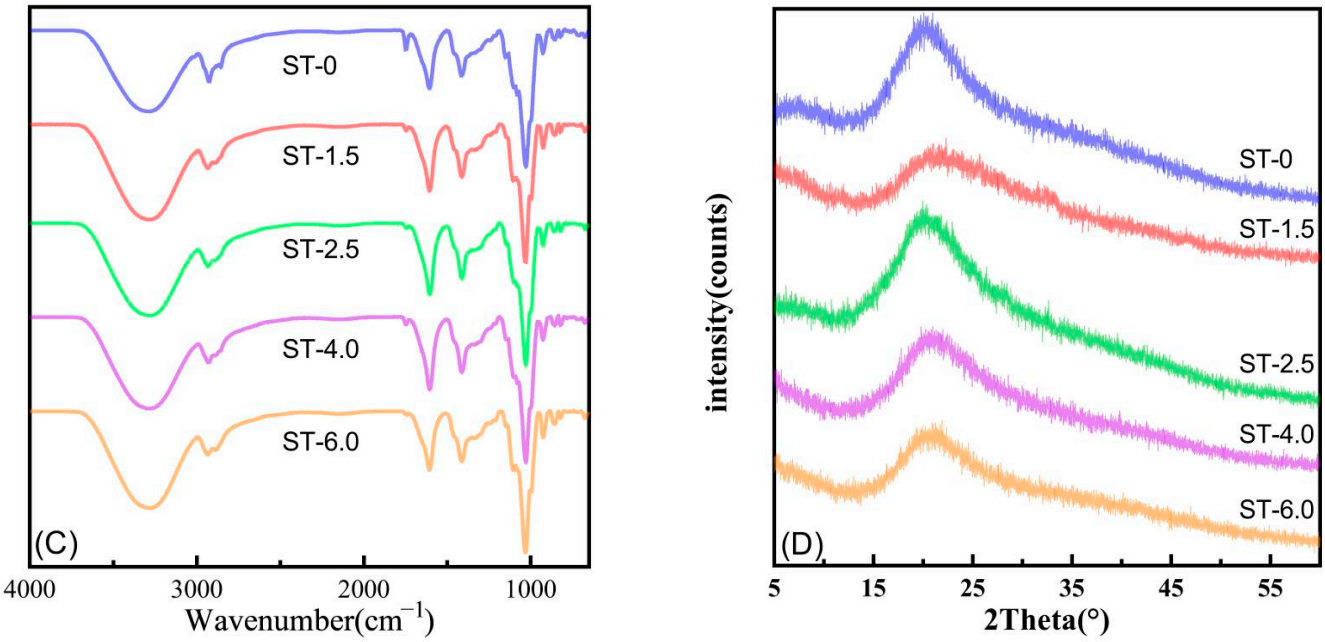

Figure 3. (**A**) The water vapor permeability of the ST films; (**B**) the oxygen permeability of the ST films; (**C**) the FTIR spectrum of the ST films; (**D**) X-ray diffraction patterns of the ST films. Different lowercase letters in the same column indicate significant differences between groups ($p < 0.05$).

3.7. FTIR Analysis

FTIR analysis is used to study the interactions between molecules in film materials. Figure 3C shows the FTIR spectrum of ST composite films. The peaks at 3300 cm^{-1} in the films were attributed to the stretching vibration of O–H and –NH [37]. In addition, due to the hydrogen bond interaction between TP and the matrix, an increase in TP concentration resulted in the migration of the N-H group at 3300 cm^{-1} towards a lower wavenumber. The peak from 2923 cm^{-1} to 2933 cm^{-1} is related to the stretching of C-H bonds. The two peaks in the range of 1348 cm^{-1}–1547 cm^{-1} are caused by the stretching of C-N and NH (amide II) and the C-O (carbonyl) vibrations, respectively [44]. After the addition of TP, the peak intensity at 1028 cm^{-1} decreased and shifted towards a higher wavenumber. These changes may be attributed to the interaction between the hydroxyl or amino groups in the matrix and the polyphenols of TP, which lead to the formation of a large number of hydrogen bonds between the functional groups [45]. Some studies have shown that the hydrogen bonds formed between phenolic compounds and polysaccharides are strong and weaken the chemical bonding force between polysaccharides, resulting in a decrease in peak intensity and the formation of a more stable edible film [46]. It is noteworthy that the spectral band near 1547 cm^{-1} was attributed to the bending vibration of absorbed water in the amorphous region of SSOS [47]. Obviously, due to the presence of TP, these bands shifted to lower frequencies. One possible explanation for this change was that, due to the hydrophilicity of TP, it significantly altered the state of water molecules in the starch matrix and formed new hydrogen bonds with water molecules [48].

3.8. XRD Analysis

XRD analysis was used to study the crystalline morphology of ST films and revealed the intermolecular interactions between the components in the ST films (Figure 3D). The broad peak at 2θ = 20.4° for all ST films indicated the amorphous structure of the matrix. After adding 2.5 wt.% TP, the characteristic peak at 2θ was strengthened. The van der Waals forces and hydrogen bonds between TP and the matrix caused the rearrangement of the polymer structure, inhibiting the crystallization process and affecting the stability of ST

films [47]. Previous studies have reported the effect of glycerol concentration on matrix crystallization, where an increase in glycerol concentration led to a decrease in the degree of crystallization [49]. The composite film showed only one diffraction peak at 20.4°, and after adding TP, the peak width increased, indicating a decrease in matrix crystallinity [35,50].

3.9. TGA

Thermogravimetric analysis is a tool used to measure the thermal properties and weight–temperature curve of materials [14]. The thermal decomposition of ST films can be divided into three stages. The first stage occurred at 60~150 °C, where the weight loss was attributed to the hydrogen bonds between the molecules inside the film being broken, and the evaporation of adsorbed and bound water in the film [51]. The second stage occurred at 170~300 °C and was related to the degradation of glycerol and some low-molecular-weight compounds in the film [52]. The third stage was above 300 °C, where polysaccharides started to depolymerize and carbonize. As shown in Figure 4, the addition of TP had a certain effect on the weight loss rate of ST films, especially in the third stage. Compared with ST-0 film, the films containing TP had a lower weight loss rate, indicating that the addition of TP may enhance the interaction between the molecules inside the ST films' matrix [18].

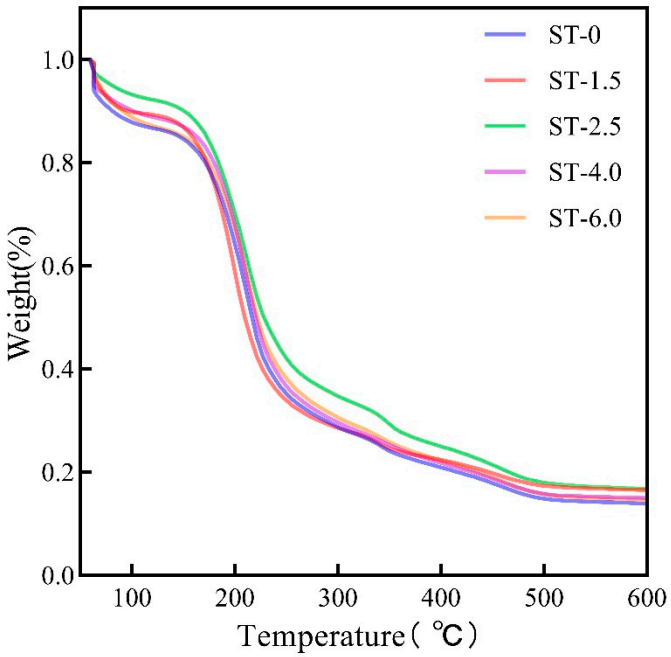

Figure 4. TGA spectrum of ST films.

3.10. SEM Analysis

The surface and cross-sectional structures of ST films were also observed by SEM, and the results are shown in Figure 5. The surface of ST-0 film was relatively smooth, with no obvious cracks or pores, and after adding TP, the surface of the composite film did not show significant changes. However, some uniform crosslinking structures appeared on the cross-section of ST films (Figure 5). This may be attributed to the partial aggregation of TP within the matrix and an increase in the hydrogen bonds between the molecules inside the matrix [53]. When the TP concentration continued to increase, particles appeared on the surface of the composite film, which may be related to the dispersion of TP in the film matrix [54].

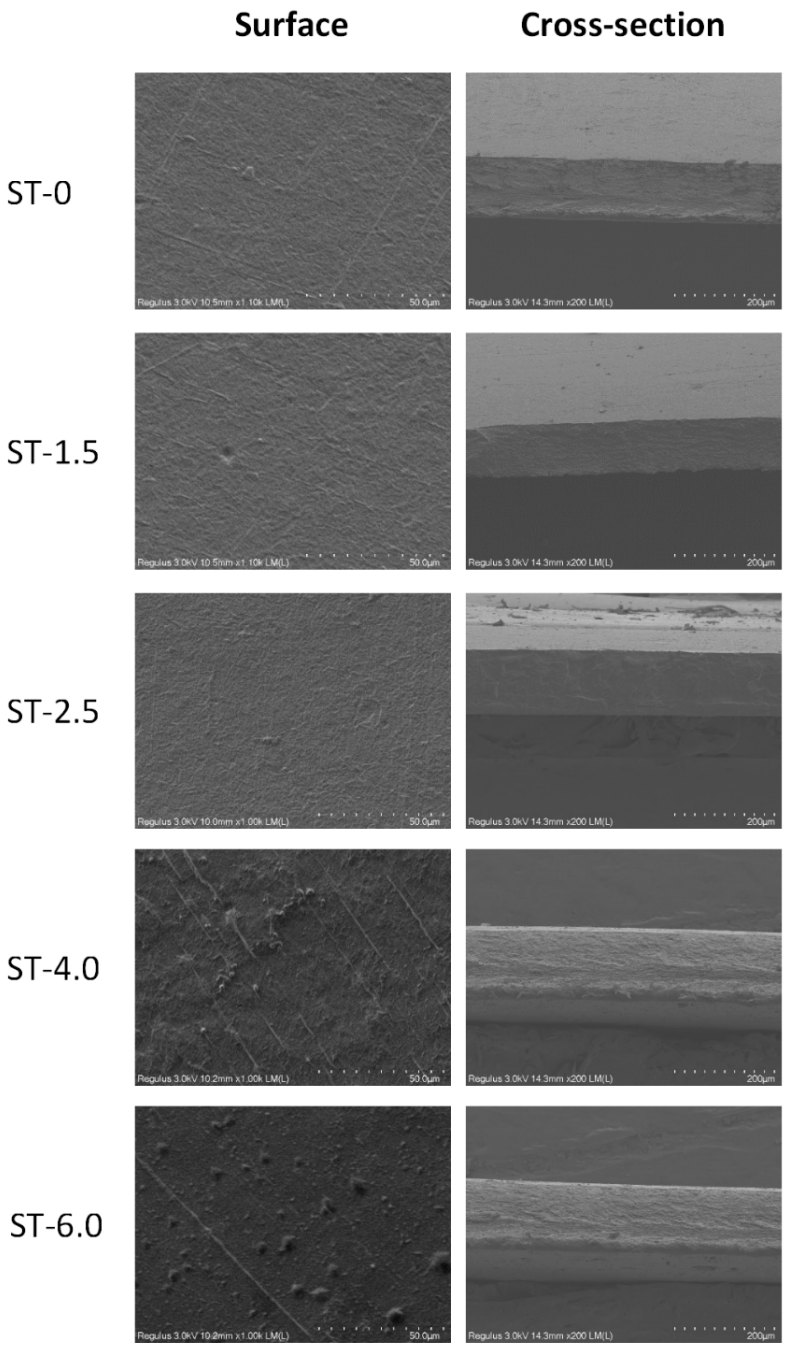

Figure 5. Surface and cross-sectional SEM micrographs of ST films.

3.11. Antioxidant Activity

The antioxidant activity of the films was evaluated using free radical scavenging assay [55]. The antioxidant activity displayed by the membrane without added TP may mainly come from the flavonoids and squalene found in the SOB [14]. The addition of TP significantly increased the scavenging ability, and this change was closely related to the concentration of TP. The TP structure contained phenolic hydroxyl groups which can effectively provide hydrogen to free radicals, thereby interrupting the chain reaction of free radicals [56]. As the TP content increased, the antioxidant capacity of ST films also improved. Compared with ST-0, ST-6.0 exhibited the highest free radical scavenging activities for both DPPH and ABTS, with a nearly 7-fold and 4-fold increase, separately ($p < 0.05$) (Figure 6A,B).

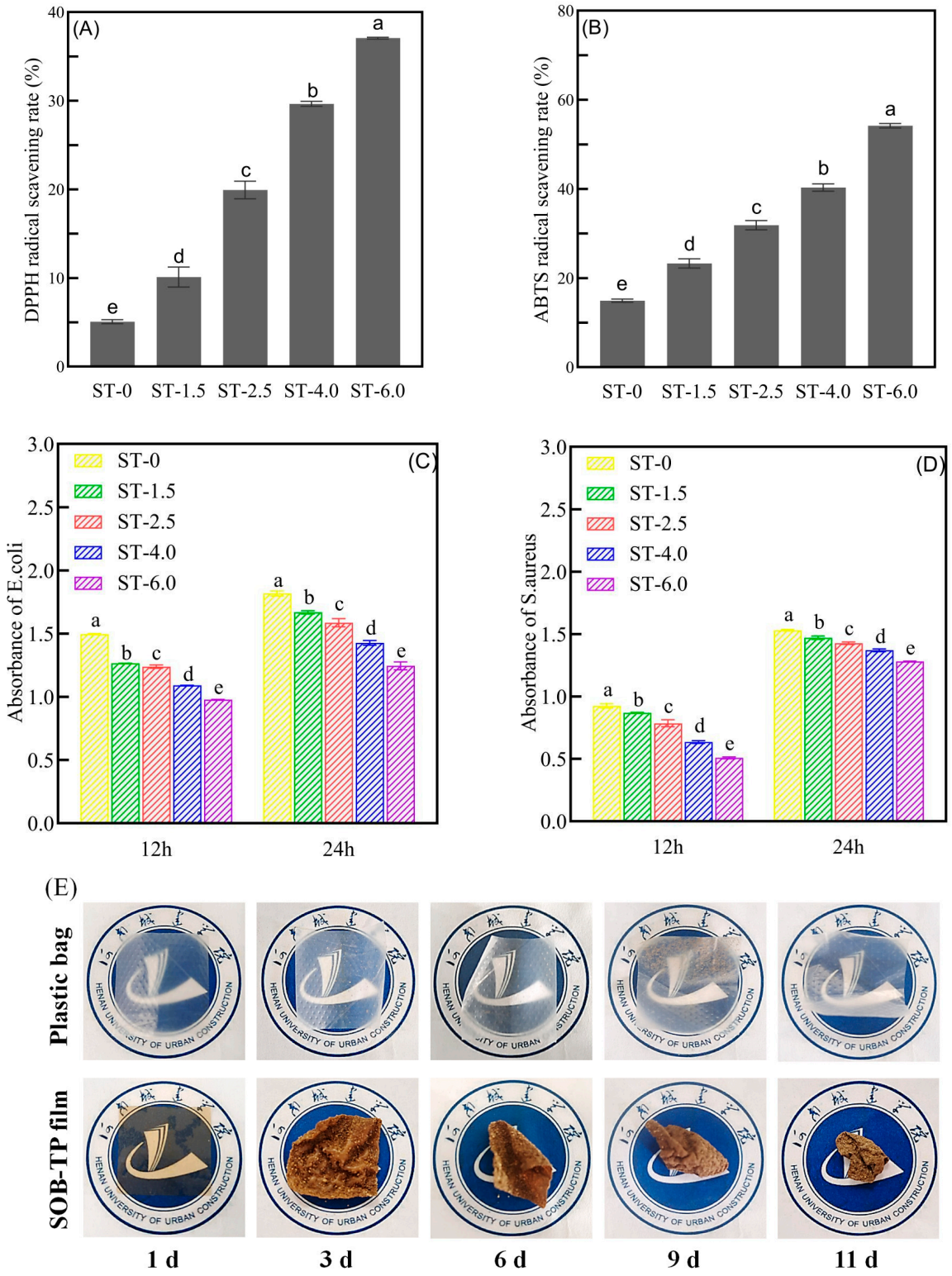

Figure 6. (**A**) The DPPH radical scavenging activity of the ST films; (**B**) the ABTS radical scavenging activity of the ST films; (**C**) the antibacterial effects of ST films on *Escherichia coli* (*E. coli*) within 24 h and 48 h with different concentrations of tea polyphenol (TP); (**D**) the antibacterial effects of ST films on *Staphylococcus aureus* (*S. aureus*) within 24 h and 48 h with different concentrations of tea polyphenol (TP); (**E**) a comparison of the degradation effects between the polyethylene film (plastic bag) and the ST-2.5 film. Different lowercase letters in the same column indicate significant differences between groups ($p < 0.05$).

3.12. Antibacterial Activity

The antibacterial activity of ST films is shown in Figure 6C,D. The addition of TP significantly enhanced the antibacterial activity of the composite film against the two bacteria ($p < 0.05$). The catechins in TP exhibited a direct antibacterial effect by disrupting the cell membrane permeability, inhibiting the synthesis of fatty acids and enzyme activity [57]. The antibacterial efficiency against *Staphylococcus aureus* (G+) is higher than that against *Escherichia coli* (G−). The lipopolysaccharide on the cell wall of *E. coli* exhibits stronger resistance against TP, while *S. aureus* is more sensitive to TP, showing strong inhibitory effects even after 24 h. Araghizadeh et al. also reported similar results, and they believed that polyphenols exhibit greater inhibitory effects on Gram-positive bacteria than on Gram-negative bacteria [58].

3.13. Biodegradability Evaluation

Degradability is an important indicator for evaluating whether bio-based films are environmentally friendly [59]. Figure 6E shows the degradation of the ST film buried in soil for 11 days. On the third day, ST film appeared wrinkled and shrunk, and on the eleventh day, due to microbial degradation and dissolution by soil moisture, most of the ST film had degraded, while the polyethylene film group remained unchanged. The results indicated that, compared to polyethylene plastic film, ST film had good degradability, which aligned with the findings of Liu et al. [53].

4. Conclusions

In this study, SOB, SA, and SSOS were used as raw materials to prepare emulsion films with TP concentrations of 0 wt.%, 1.5 wt.%, 2.5 wt.%, 4.0 wt.%, and 6.0 wt.%, respectively. The ST film exhibited favorable physical properties, and antibacterial and antioxidant activities. Overall, ST-2.5 combination was the best, as the ST film showed optimal mechanical and barrier properties at this concentration. FTIR results indicated that polyphenols formed new hydrogen bonds with the film matrix. However, when the TP concentration increased to 4.0 wt.%, SEM results showed that TP may exist in the form of free particles, which could affect the physicochemical properties of the film, such as with a decrease in tensile strength and water resistance. In summary, ST film was observed a new antibacterial, antioxidant, and edible film, which can serve as a functional food packaging material. The results of this study will promote the research and development of functional oil-in-water (O/W) emulsion films and enable the development of new opportunities for O/W emulsion films in the food packaging industry. Moreover, we look forward to exploring the potential application of other types of oil body materials or substances that can improve the functionality of the film as a film-forming matrix for biodegradable films.

Author Contributions: J.S.: writing—original draft preparation, investigation, methodology. L.W.: data curation, software, methodology. H.C.: data curation, formal analysis. G.Y.: conceptualization, writing—review and editing, project administration, funding acquisition. All authors have read and agreed to the published version of the manuscript.

Funding: The authors would like to thank the funding provided by the Pingdingshan Science and Technology Innovation Outstanding Talents Program (2017010(10.4)); the funding provided by the Key Scientific and Technological Project of Henan Province (No. 232102110087), and the funding provided by Henan Key Scientific Research Projects (No. 25B550022).

Institutional Review Board Statement: Not applicable.

Informed Consent Statement: Not applicable.

Data Availability Statement: No data were used for the research described in the article.

Conflicts of Interest: The authors declare no conflict of interest.

References

1. Sundqvist-Andberg, H.; Åkerman, M. Sustainability governance and contested plastic food packaging—An integrative review. *J. Clean. Prod.* **2021**, *306*, 127111. [CrossRef]
2. Mohamed, S.A.A.; El-Sakhawy, M.; El-Sakhawy, M.A.M. Polysaccharides, Protein and Lipid -Based Natural Edible Films in Food Packaging: A Review. *Carbohydr. Polym.* **2020**, *238*, 116178. [CrossRef]
3. Gooneh-Farahani, S.; Naimi-Jamal, M.R.; Naghib, S.M. Stimuli-responsive graphene-incorporated multifunctional chitosan for drug delivery applications: A review. *Expert Opin. Drug Deliv.* **2018**, *16*, 79–99. [CrossRef]
4. Jiang, Y.; Lan, W.; Sameen, D.E.; Ahmed, S.; Qin, W.; Zhang, Q.; Chen, H.; Dai, J.; He, L.; Liu, Y. Preparation and characterization of grass carp collagen-chitosan-lemon essential oil composite films for application as food packaging. *Int. J. Biol. Macromol.* **2020**, *160*, 340–351. [CrossRef]
5. Ran, R.; Zheng, T.; Tang, P.; Xiong, Y.; Yang, C.; Gu, M.; Li, G. Antioxidant and antimicrobial collagen films incorporating Pickering emulsions of cinnamon essential oil for pork preservation. *Food Chem.* **2023**, *420*, 136108. [CrossRef]
6. Perdones, Á.; Chiralt, A.; Vargas, M. Properties of film-forming dispersions and films based on chitosan containing basil or thyme essential oil. *Food Hydrocoll.* **2016**, *57*, 271–279. [CrossRef]
7. Xu, Y.; Chu, Y.; Feng, X.; Gao, C.; Wu, D.; Cheng, W.; Meng, L.; Zhang, Y.; Tang, X. Effects of zein stabilized clove essential oil Pickering emulsion on the structure and properties of chitosan-based edible films. *Int. J. Biol. Macromol.* **2020**, *156*, 111–119. [CrossRef] [PubMed]
8. Matsakidou, A.; Biliaderis, C.G.; Kiosseoglou, V. Preparation and characterization of composite sodium caseinate edible films incorporating naturally emulsified oil bodies. *Food Hydrocoll.* **2013**, *30*, 232–240. [CrossRef]
9. Ma, Q.; Zhang, Y.; Critzer, F.; Davidson, P.M.; Zivanovic, S.; Zhong, Q. Physical, mechanical, and antimicrobial properties of chitosan films with microemulsions of cinnamon bark oil and soybean oil. *Food Hydrocoll.* **2016**, *52*, 533–542. [CrossRef]
10. Shimada, T.L.; Hayashi, M.; Hara-Nishimura, I. Membrane Dynamics and Multiple Functions of Oil Bodies in Seeds and Leaves. *Plant Physiol.* **2017**, *176*, 199–207. [CrossRef]
11. Şen, A.; Acevedo-Fani, A.; Dave, A.; Ye, A.; Husny, J.; Singh, H. Plant oil bodies and their membrane components: New natural materials for food applications. *Crit. Rev. Food Sci. Nutr.* **2022**, *64*, 256–279. [CrossRef]
12. Nikiforidis, C.V. Structure and functions of oleosomes (oil bodies). *Adv. Colloid Interface Sci.* **2019**, *274*, 102039. [CrossRef] [PubMed]
13. Wang, L. Properties of Soybean Oil Bodies and Oleosin Proteins as Edible Films and Coatings. Ph.D. Dissertation, Purdue University, West Lafayette, IN, USA, 2004.
14. Sun, J.; Wang, L.; Chen, H.; Yin, G. Preparation and application of edible film based on sodium carboxymethylcellulose-sodium alginate composite soybean oil body. *Coatings* **2023**, *13*, 1716. [CrossRef]
15. Kuai, L.; Liu, F.; Ma, Y.; Goff, H.D.; Zhong, F. Regulation of nano-encapsulated tea polyphenol release from gelatin films with different Bloom values. *Food Hydrocoll.* **2020**, *108*, 106045. [CrossRef]
16. Dai, J.; Sameen, D.E.; Zeng, Y.; Li, S.; Qin, W.; Liu, Y. An overview of tea polyphenols as bioactive agents for food packaging applications. *LWT* **2022**, *167*, 113845. [CrossRef]
17. Zhang, W.; Jiang, H.; Rhim, J.-W.; Cao, J.; Jiang, W. Tea polyphenols (TP): A promising natural additive for the manufacture of multifunctional active food packaging films. *Crit. Rev. Food Sci. Nutr.* **2021**, *63*, 288–301. [CrossRef]
18. Zhou, X.; Liu, X.; Wang, Q.; Lin, G.; Yang, H.; Yu, D.; Cui, S.W.; Xia, W. Antimicrobial and antioxidant films formed by bacterial cellulose, chitosan and tea polyphenol—Shelf life extension of grass carp. *Food Packag. Shelf Life* **2022**, *33*, 100866. [CrossRef]
19. Wu, N.-N.; Huang, X.; Yang, X.-Q.; Guo, J.; Zheng, E.-L.; Yin, S.-W.; Zhu, J.-H.; Qi, J.-R.; He, X.-T.; Zhang, J.-B. Stabilization of soybean oil body emulsions using ι-carrageenan: Effects of salt, thermal treatment and freeze-thaw cycling. *Food Hydrocoll.* **2011**, *28*, 110–120. [CrossRef]
20. Moghadam, M.; Salami, M.; Mohammadian, M.; Khodadadi, M.; Emam-Djomeh, Z. Development of antioxidant edible films based on mung bean protein enriched with pomegranate peel. *Food Hydrocoll.* **2020**, *104*, 105735. [CrossRef]
21. Choi, I.; Shin, D.; Lyu, J.S.; Lee, J.-S.; Song, H.-G.; Chung, M.-N.; Han, J. Physicochemical properties and solubility of sweet potato starch-based edible films. *Food Packag. Shelf Life* **2022**, *33*, 100867. [CrossRef]
22. Wu, H.; Li, T.; Peng, L.; Wang, J.; Lei, Y.; Li, S.; Li, Q.; Yuan, X.; Zhou, M.; Zhang, Z. Development and characterization of antioxidant composite films based on starch and gelatin incorporating resveratrol fabricated by extrusion compression moulding. *Food Hydrocoll.* **2023**, *139*, 108509. [CrossRef]
23. Tan, L.F.; Elaine, E.; Pui, L.P.; Nyam, K.L.; Aniza, Y. Development of chitosan edible film incorporated with Chrysanthemum morifolium essential oil. *Acta Sci. Pol. Technol. Aliment.* **2021**, *20*, 55–66. [CrossRef] [PubMed]
24. Bhopal, R.R.L. Investigation of water vapour permeation and antibacterial properties of nano silver loaded cellulose acetate film. *Int. Food Res. J.* **2010**, *17*, 623–639.

25. Sun, R.; Zhu, J.; Wu, H.; Wang, S.; Li, W.; Sun, Q. Modulating layer-by-layer assembled sodium alginate-chitosan film properties through incorporation of cellulose nanocrystals with different surface charge densities. *Int. J. Biol. Macromol.* **2021**, *180*, 510–522. [CrossRef] [PubMed]
26. Kim, S.; Baek, S.K.; Go, E.; Song, K.B. Application of adzuki bean starch in antioxidant films containing cocoa nibs extract. *Polymers* **2018**, *10*, 1210. [CrossRef]
27. Yuan, L.; Feng, W.; Zhang, Z.; Peng, Y.; Xiao, Y.; Chen, J. Effect of potato starch-based antibacterial composite films with thyme oil microemulsion or microcapsule on shelf life of chilled meat. *LWT-Food Sci. Technol.* **2021**, *139*, 110462. [CrossRef]
28. Zhao, Y.; Du, J.; Zhou, H.; Zhou, S.; Lv, Y.; Cheng, Y.; Tao, Y.; Lu, J.; Wang, H. Biodegradable intelligent film for food preservation and real-time visual detection of food freshness. *Food Hydrocoll.* **2022**, *129*, 107665. [CrossRef]
29. Zhang, W.; Jiang, W. Antioxidant and antibacterial chitosan film with tea polyphenols-mediated green synthesis silver nanoparticle via a novel one-pot method. *Int. J. Biol. Macromol.* **2020**, *155*, 1252–1261. [CrossRef]
30. Jamróz, E.; Kulawik, P.; Krzyściak, P.; Talaga-Ćwiertnia, K.; Juszczak, L. Intelligent and active furcellaran-gelatin films containing green or pu-erh tea extracts: Characterization, antioxidant and antimicrobial potential. *Int. J. Biol. Macromol.* **2019**, *122*, 745–757. [CrossRef] [PubMed]
31. Wu, Z.; Li, Y.; Tang, J.; Lin, D.; Qin, W.; A Loy, D.; Zhang, Q.; Chen, H.; Li, S. Ultrasound-assisted preparation of chitosan/nano-silica aerogel/tea polyphenol biodegradable films: Physical and functional properties. *Ultrason. Sonochemistry* **2022**, *87*, 106052. [CrossRef]
32. Vargas, M.; Perdones, Á.; Chiralt, A.; Cháfer, M.; González-Martínez, C. Effect of homogenization conditions on physicochemical properties of chitosan-based film-forming dispersions and films. *Food Hydrocoll.* **2011**, *25*, 1158–1164. [CrossRef]
33. Liu, Y.; Wang, S.; Lan, W.; Qin, W. Development of ultrasound treated polyvinyl alcohol/tea polyphenol composite films and their physicochemical properties. *Ultrason. Sonochemistry* **2019**, *51*, 386–394. [CrossRef] [PubMed]
34. Feng, M.; Yu, L.; Zhu, P.; Zhou, X.; Liu, H.; Yang, Y.; Zhou, J.; Gao, C.; Bao, X.; Chen, P. Development and preparation of active starch films carrying tea polyphenol. *Carbohydr. Polym.* **2018**, *196*, 162–167. [CrossRef]
35. Gao, L.; Zhu, T.; He, F.; Ou, Z.; Xu, J.; Ren, L. Preparation and characterization of functional films based on chitosan and corn starch incorporated tea polyphenols. *Coatings* **2021**, *11*, 817. [CrossRef]
36. Zhao, Q.; Xu, Y.; Liu, Y. Soybean oil bodies: A review on composition, properties, food applications, and future research aspects. *Food Hydrocoll.* **2022**, *124*, 107296. [CrossRef]
37. Biao, Y.; Yuxuan, C.; Qi, T.; Ziqi, Y.; Yourong, Z.; McClements, D.J.; Chongjiang, C. Enhanced performance and functionality of active edible films by incorporating tea polyphenols into thin calcium alginate hydrogels. *Food Hydrocoll.* **2019**, *97*, 105197. [CrossRef]
38. Guzman-Puyol, S.; Benitez, J.J.; Heredia-Guerrero, J.A. Transparency of polymeric food packaging materials. *Food Res. Int.* **2022**, *161*, 111792. [CrossRef] [PubMed]
39. Rukmanikrishnan, B.; Kim, S.S.; Lee, J.; Lee, J. Effect of TiO_2 on highly elastic, stretchable UV protective nanocomposite films formed by using a combination of k-Carrageenan, xanthan gum and gellan gum. *Int. J. Biol. Macromol.* **2019**, *123*, 1020–1027. [CrossRef]
40. Yildirim, S.; Röcker, B.; Pettersen, M.K.; Nilsen-Nygaard, J.; Ayhan, Z.; Rutkaite, R.; Radusin, T.; Suminska, P.; Marcos, B.; Coma, V. Active packaging applications for food. *Compr. Rev. Food Sci. Food Saf.* **2018**, *17*, 165–199. [CrossRef] [PubMed]
41. Cazón, P.; Velázquez, G.; Vázquez, M. Characterization of bacterial cellulose films combined with chitosan and polyvinyl alcohol: Evaluation of mechanical and barrier properties. *Carbohydr. Polym.* **2019**, *216*, 72–85. [CrossRef] [PubMed]
42. Dong, M.; Tian, L.; Li, J.; Jia, J.; Dong, Y.; Tu, Y.; Liu, X.; Tan, C.; Duan, X. Improving physicochemical properties of edible wheat gluten protein films with proteins, polysaccharides and organic acid. *LWT-Food Sci. Technol.* **2022**, *154*, 112868. [CrossRef]
43. Wang, X.; Huang, X.; Zhang, F.; Hou, F.; Yi, F.; Sun, X.; Yang, Q.; Han, X.; Liu, Z. Characterization of chitosan/zein composite film combined with tea polyphenol and its application on postharvest quality improvement of mushroom (Lyophyllum decastes Sing). *Food Packag. Shelf Life* **2022**, *33*, 100869. [CrossRef]
44. Zhou, X.; Liu, X.; Liao, W.; Wang, Q.; Xia, W. Chitosan/bacterial cellulose films incorporated with tea polyphenol nanoliposomes for silver carp preservation. *Carbohydr. Polym.* **2022**, *297*, 120048. [CrossRef] [PubMed]
45. Gao, H.X.; He, Z.; Sun, Q.; He, Q.; Zeng, W.C. A functional polysaccharide film forming by pectin, chitosan, and tea polyphenols. *Carbohydr. Polym.* **2019**, *215*, 1–7. [CrossRef] [PubMed]
46. Lee, H.; Rukmanikrishnan, B.; Lee, J. Rheological, morphological, mechanical, and water-barrier properties of agar/gellan gum/montmorillonite clay composite films. *Int. J. Biol. Macromol.* **2019**, *141*, 538–544. [CrossRef]
47. Kizil, R.; Irudayaraj, J.; Seetharaman, K. Characterization of irradiated starches by using FT-Raman and FTIR spectroscopy. *J. Agric. Food Chem.* **2002**, *50*, 3912–3918. [CrossRef] [PubMed]
48. Aresta, A.; Calvano, C.D.; Trapani, A.; Cellamare, S.; Zambonin, C.G.; De Giglio, E. Development and analytical characterization of vitamin (s)-loaded chitosan nanoparticles for potential food packaging applications. *J. Nanoparticle Res.* **2013**, *15*, 1–12. [CrossRef]

49. Liu, H.; Adhikari, R.; Guo, Q.; Adhikari, B. Preparation and characterization of glycerol plasticized (high-amylose) starch–chitosan films. *J. Food Eng.* **2013**, *116*, 588–597. [CrossRef]
50. Wu, Y.; Chen, Z.X.; Li, X.X.; Li, M. Effect of tea polyphenols on the retrogradation of rice starch. *Food Res. Int.* **2009**, *42*, 221–225. [CrossRef]
51. Nguyen, T.T.; Pham BT, T.; Le, H.N.; Bach, L.G.; Thuc, C.H. Comparative characterization and release study of edible films of chitosan and natural extracts. *Food Packag. Shelf Life* **2022**, *32*, 100830. [CrossRef]
52. Oluwasina, O.O.; Olaleye, F.K.; Olusegun, S.J.; Oluwasina, O.O.; Mohallem, N.D. Influence of oxidized starch on physicomechanical, thermal properties, and atomic force micrographs of cassava starch bioplastic film. *Int. J. Biol. Macromol.* **2019**, *135*, 282–293. [CrossRef]
53. Liu, J.; Wang, Y.; Lv, J.; Wu, Y.; Guo, Y.; Sun, C.; Li, X. Biodegradable composite films based on egg white protein and tea polyphenol: Physicochemical, structural and antibacterial properties. *Food Packag. Shelf Life* **2023**, *38*, 101098. [CrossRef]
54. Xu, J.; Xia, R.; Yuan, T.; Sun, R. Use of xylooligosaccharides (XOS) in hemicelluloses/chitosan-based films reinforced by cellulose nanofiber: Effect on physicochemical properties. *Food Chem.* **2019**, *298*, 125041. [CrossRef] [PubMed]
55. Rumpf, J.; Burger, R.; Schulze, M. Statistical evaluation of DPPH, ABTS, FRAP, and Folin-Ciocalteu assays to assess the antioxidant capacity of lignins. *Int. J. Biol. Macromol.* **2023**, *233*, 123470. [CrossRef]
56. Yan, Z.; Zhong, Y.; Duan, Y.; Chen, Q.; Li, F. Antioxidant mechanism of tea polyphenols and its impact on health benefits. *Anim. Nutr.* **2020**, *6*, 115–123. [CrossRef] [PubMed]
57. Reygaert, W.; Jusufi, I. Green tea as an effective antimicrobial for urinary tract infections caused by *Escherichia coli*. *Front. Microbiol.* **2013**, *4*, 162. [CrossRef] [PubMed]
58. Araghizadeh, A.; Kohanteb, J.; Fani, M.M. Inhibitory activity of green tea (*Camellia sinensis*) extract on some clinically isolated cariogenic and periodontopathic bacteria. *Med. Princ. Pract.* **2013**, *22*, 368–372. [CrossRef] [PubMed]
59. Nigam, S.; Das, A.K.; Patidar, M.K. Synthesis, characterizationand biodegradation of bioplastic films produced from Parthenium hysterophorus by incorporating a plasticizer (PEG600). *Environ. Chall.* **2021**, *5*, 100280. [CrossRef]